THE PROTEIN SOCIETY

Hydrogen exchange of disordered proteins in *Escherichia coli*

Austin E. Smith,[1] Larry Z. Zhou,[1] and Gary J. Pielak[1,2,3]*

[1]Department of Chemistry, University of North Carolina, Chapel Hill, North Carolina 27599
[2]Department of Biochemistry and Biophysics, University of North Carolina, Chapel Hill, North Carolina 27599
[3]Lineberger Comprehensive Cancer Center, University of North Carolina, Chapel Hill, North Carolina 27599

Received 15 January 2015; Accepted 16 January 2015
DOI: 10.1002/pro.2643
Published online 21 January 2015 proteinscience.org

Abstract: A truly disordered protein lacks a stable fold and its backbone amide protons exchange with solvent at rates predicted from studies of unstructured peptides. We have measured the exchange rates of two model disordered proteins, FlgM and α-synuclein, in buffer and in *Escherichia coli* using the NMR experiment, SOLEXSY. The rates are similar in buffer and cells and are close to the rates predicted from data on small, unstructured peptides. This result indicates that true disorder can persist inside the crowded cellular interior and that weak interactions between proteins and macromolecules in cells do not necessarily affect intrinsic rates of exchange.

Keywords: amide proton exchange; intrinsically disordered proteins; in-cell NMR; SOLEXSY; macromolecular crowding

Introduction

Cellular processes occur at macromolecule concentrations of 300–400 g/L.[1,2] The resulting weak, nonspecific interactions between macromolecules in the cytoplasm alter globular protein dynamics and stability.[3–6] Disordered proteins are fundamentally different. Unlike many model, single domain, globular proteins, whose structures do not change until they denature,[7] the properties of disordered proteins depend on solution conditions.[8] Thus, the crowded nature of the cell could have large effects on protein disorder. Studies show that the cellular interior can promote structure formation in proteins that are only transiently structured in buffer.[9] On the other hand, there is a growing realization from studies of globular proteins that attractive interactions favor less structure.[10–16]

To date, knowledge of the atomic-level structure of disordered proteins inside cells comes from crude measures: the presence or absence of crosspeaks in ^{15}N-^{1}H HSQC NMR spectra and chemical shifts.[9,17] Absence of peaks is caused by chemical exchange and is explained in contrasting ways: (1) intramolecular exchange involving the stabilization of particular conformations (i.e., folded species) and (2) weak, transient chemical interactions between the test protein and cellular components.[9,18–20] Here, we take a new approach by quantifying hydrogen exchange rates for two proteins possessing different degrees of disorder.

Structure protects backbone amide protons from solvent exchange.[21] Therefore, measuring their exchange rates inside cells and comparing the values to those measured in buffer and calculated from unstructured peptides provides information about structure. Protection is quantified as the rate in an unstructured peptide ($\sim 0.1 - 10\ s^{-1}$)[22] divided by the observed rate, k_{int}/k_{obs}. These protection factors

Abbreviations: CLEANEX, phase-modulated CLEAN chemical exchange; HSQC, heteronuclear single quantum correlation; Nat, N-α-acetyltransferase; NMR, nuclear magnetic resonance; SOLEXSY, solvent exchange spectroscopy

Additional Supporting Information may be found in the online version of this article.

Grant sponsor: National Science Foundation; Grant numbers: MCB 1051819, MCB 1410854.

*Correspondence to: Gary J. Pielak, Department of Chemistry, University of North Carolina, Chapel Hill, NC 27599-3290. E-mail: gary_pielak@unc.edu

range from $>10^5$ for backbone amide protons in the core of globular proteins to <5 for denatured proteins.[5,10,23] Intrinsic rates in buffer are estimated by using the online program, SPHERE,[24] which calculates k_{int} based on data from unstructured peptides and information about the system (i.e., primary structure, pH, deuterium content, and temperature).[22,25] These calculated rates remain valid in buffers containing physiologically relevant concentrations of globular proteins and cell lysates.[11,26]

Direct measurement of exchange in cells, however, is challenging. We investigated the disordered proteins α-synuclein and FlgM, both of which give in-cell NMR spectra,[9,18,27,28] using the SOLEXSY experiment[26,29] to quantify k_{obs} in *Escherichia coli* and buffer. SOLEXSY uses a variable mixing time (t_{mix}) to monitor hydrogen exchange (Supporting Information Fig. S1). Short times do not result in a buildup crosspeak. Longer times allow amide deuterons to exchange for protons and buildup of the initially deuterated amide crosspeak occurs. Similarly, a decay is observed from the initially protonated species. Rates are obtained from fits of peak volume versus mixing time.

α-Synuclein is a 140-residue protein found at the presynaptic terminals of neurons.[30] Its exact role is controversial, but the protein is *N*-terminally acetylated and thought to play a part in dopamine trafficking.[8] α-Synuclein retains the majority of its ^{15}N-^{1}H correlation crosspeaks inside *E. coli*, suggesting that the protein remains disordered in cells.[17,18,27,28]

FlgM is a 97-residue protein from *Salmonella typhimurium* that inhibits σ^{28}, a transcription factor responsible for regulating downstream flagellar and chemotaxis genes.[31,32] The protein shows characteristics of both a globular and a disordered protein. The *C*-terminus (residues 41–97) forms transient helices in buffer (between residues 60–73 and 83–90).[33] These helices are stabilized upon binding σ^{28}.[34] The absence of crosspeaks from the ^{15}N-^{1}H correlation spectrum for the *C*-terminal region in *E. coli* has been interpreted as evidence that this region gains structure in cells.[9] The *N*-terminus (residues 1–40) appears to remain disordered even in cells.[9,33]

Results

Amide proton exchange is base-catalyzed at physiological pH.[21,22] In-cell NMR in *E. coli* is usually performed in dense cell slurries that are inherently low in nutrients and O_2.[35,36] These anaerobic conditions cause acidification of the cellular interior.[17,37,38] Thus, the interior pH must be known to compare data obtained in cells to data obtained in buffer. α-Synuclein has a single histidine, H50, whose $^{13}C^{\epsilon 1}$ proton chemical shift depends on pH.[39] The C14 protons of HEPES, which is not cell permeable, were used as an external pH probe.[40,41] ^{13}C-^{1}H HSQC spectra were acquired before and after the SOLEXSY experiment.

The proton chemical shifts were compared to those from a standard curve in buffer (Supporting Information Figs. S2, S3). The cytoplasm and the extracellular medium acidified over the ~16 h required to acquire a SOLEXSY dataset (Supporting Information Table S1), and the internal pH was ~0.4 units lower than the external pH (Supporting Information Fig. S4). The average internal pH of all α-synuclein datasets is pH 6.7. We corrected the in-cell rates to pH 6.7 by using the second-order rate constant for base-catalyzed exchange (Supporting Information Table S2, footnotes c-e).[42] We used this corrected rate to compare intracellular hydrogen exchange rates to those measured in buffer and to drive SPHERE. Since FlgM does not have a pH sensitive probe, we measured the HEPES C14 proton chemical shift before and after the SOLEXSY experiment, and applied the 0.4 pH unit correction to determine the internal pH.

During the course of an in-cell experiment the intercellular pH typically drops below 6.5 (Supporting Information Table S1). Below this pH (at 288 K) the signal to noise ratio of buildup peaks is typically too small to allow exchange rates to be quantified, because hydrogen exchange drops below 0.1 s^{-1} for many residues. This problem is exacerbated in-cells, where peaks are inherently broad. To estimate exchange rates from crosspeaks with weak buildup curves we used a standard curve of the ratio of buildup to decay peak volumes at a t_{mix} of 0.3 s versus the k_{obs} values from the fit obtained in buffer (Supporting Information Fig. S5). This procedure allows an exchange rate to be estimated by a SOLEXSY experiment with one t_{mix}, 0.3 s. The uncertainty in this measurement was estimated as the maximum and minimum rates within 0.1 unit of the ratio.

Hydrogen exchange rates for α-synuclein and FlgM are compiled in Supporting Information Tables S3–S7. SPHERE-predicted k_{int} values match k_{obs} values in buffer for α-synuclein, acetylated α-synuclein, and FlgM. In addition, rates and protection factors for α-synuclein in buffer closely match those measured with CLEANEX (Supporting Information Table S3).[27] The differences likely reflect differences in buffer composition and extrapolation to pH 6.7.

In buffer, 26 α-synuclein residues give quantifiable exchange rates and seven more rates can be estimated [Figs. 1(A) and 2(A), Supporting Information Table S3]. The residues are distributed throughout the primary structure. Their protection factors are all similar and less than two. The same is observed for α-synuclein in buffer supplemented with 150 m*M* NaCl (Supporting Information Table S3).

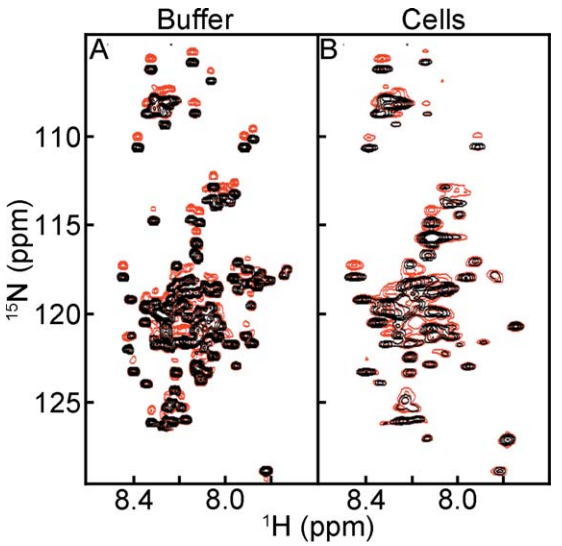

Figure 1. $^{15}N^{H/D}$-SOLEXSY spectra of α-synuclein in (A) buffer and (B) *E. coli*. Each panel is an overlay of the 0 ms (black) and 300 ms (red) mixing times. The contour levels in panels A and B are the same.

Protection factors this small indicate a lack of structure.[23]

In cells, nine α-synuclein residues give quantifiable rates, eight more rates can be estimated, and an additional six qualitatively show exchange [Figs. 1(B) and 2(A), Supporting Information Tables S2 and S3). Rates in cells and in buffer are in reasonable agreement with the values predicted by SPHERE. No protection factor is greater than three [Fig. 2(B)]. There is no significant difference between the protection factors, both measured and estimated, in cells and in buffer (two-tailed *t*-test with unequal variance,[43] $\rho > 0.07$). The same is observed for acetylated α-synuclein. There is no significant difference between protection factors in cells and buffer (Supporting Information Fig. S6, Tables S4 and S5, two-tailed *t*-test with unequal variance, $\rho > 0.5$). These observations along with chemical shift data from the protein in cells[17] indicate that α-synuclein, with or without acetylation, remains disordered in the crowded bacterial cytoplasm.

The activation energy of amide proton exchange was also measured (Supporting Information Table S8). The means and their standard deviations are 15 ± 3 kcal/mol in buffer and 17 ± 1 kcal/mol in cells. The activation energy used in SPHERE is 17 kcal/mol.[22,24] These observations lend further support our to conclusion that α-synuclein has the properties of a disordered peptide in the *E. coli* cytoplasm.

Turning to FlgM, 24 residues give quantifiable exchange rates in buffer [Figs. 3(A) and 4(A),

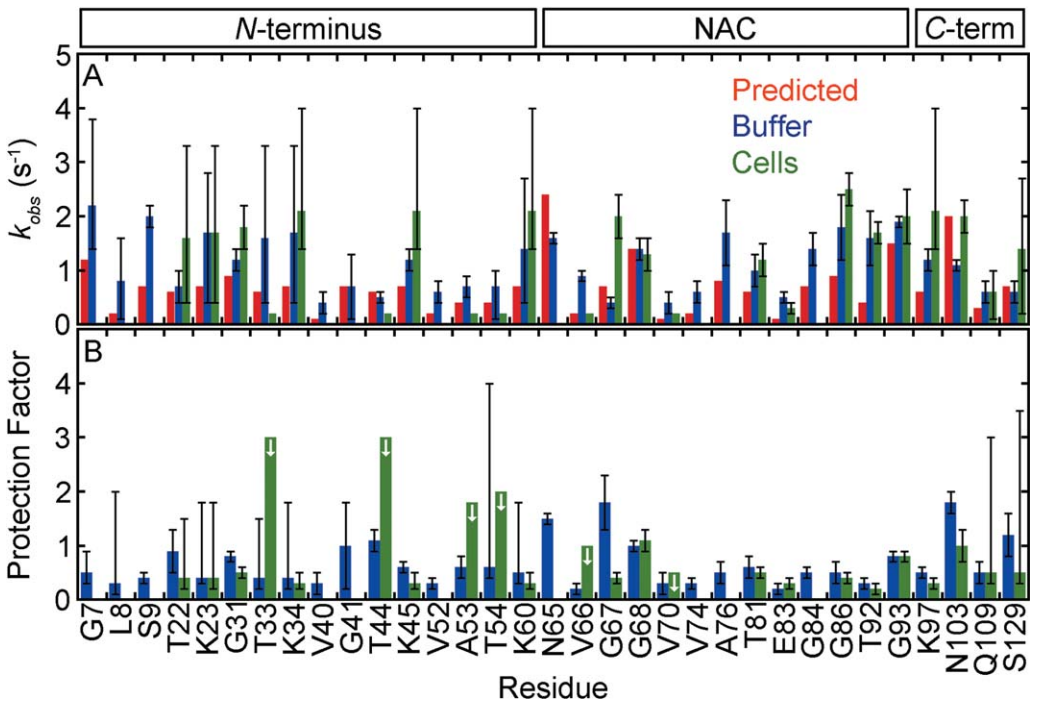

Figure 2. α-Synuclein exhibits similar backbone amide hydrogen exchange rates in cells and in buffer (pH 6.7, 288 K). (A) Rates from prediction (red),[22,24,25] and from SOLEXSY data (blue, buffer; green, cells). Uncertainties in buffer are the standard deviation of 20 Monte Carlo noise simulations.[29] Uncertainties for the in-cell data are the standard deviation of the mean from three or more trials (For T81 and G93, the uncertainties are the range of two experiments.). Asymmetric error bars are shown for rates derived from the data in Supporting Information Figure S5, as described in the text. In-cell rates without error bars are for residues that exchange too slowly for reliable fits, or have overlapped decay peaks, and were assigned a rate of ≥ 0.2 s^{-1}, the lower limit of SOLEXSY. (B) Protection factors ($k_{int,\ predicted}/k_{obs,\ buffer}$ and $k_{int,\ predicted}/k_{obs,\ cells}$). Uncertainties are from propagation of the uncertainties shown in panel A unless the rate was derived from Supporting Information Figure S5. For those residues, the uncertainty reflects a range, as described in the text. The arrows denote residues for which only a maximum value can be assigned.

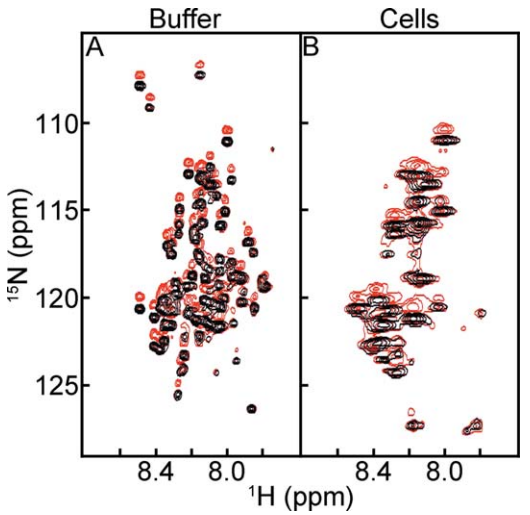

Figure 3. $^{15}N^{H/D}$-SOLEXSY spectra of FlgM in (A) buffer and (B) *E. coli*. Each panel is an overlay of the 0 ms (black) and 300 ms (red) mixing times. The contour levels in panels A and B are the same.

Supporting Information Table S7). Significantly larger protection factors ($\rho < 0.002$, two-tailed *t*-test with unequal variance) are observed for the 13 *C*-terminal residues compared to the 11 *N*-terminal residues (means and their standard deviations of 1.6 ± 0.3 and 0.5 ± 0.1, respectively). This observation suggests the existence of some structure in the *C*-terminal region, consistent with chemical-shift data showing that the *C*-terminus forms transient α-helices in buffer.[33,34] However, the protection factors from the *C*-terminal region were all <5, indicating an absence of persistent structure.[23] In summary, the agreement between the chemical-shift data and the hydrogen exchange data show that protection factors are a sensitive measure of sparsely populated secondary structure.

In cells, seven FlgM residues give quantifiable rates and four more qualitatively show exchange [Figs. 3(B) and 4(A), Supporting Information Tables S6 and S7]. The rates in cells are similar to those in buffer. For the *N*-terminus seven residues can be quantified in cells and 11 in buffer. Protection factors for these residues [Fig. 4(B)] are the same in cells as they are in buffer (two-tailed *t*-test with unequal variance, $\rho > 0.1$).

Discussion

Our data for α-synuclein and the *N*-terminal region of FlgM indicate that disorder can persist in *E. coli* irrespective of the existence of hard-core repulsions, i.e. macromolecular crowding.[3,4] We cannot directly compare cell and buffer data from the *C*-terminus of FlgM because *C*-terminal crosspeaks disappear in cells.[9] However, the smaller exchange rates in buffer and the absence of crosspeaks are both consistent with the existence of a nascent *C*-terminal structure. Likewise, for both acetylated and non-acetylated α-synuclein, crosspeaks from the first 12 residues and residues 37–41 show peak broadening inside cells (Supporting Information Fig. S7). This broadening is likely due to conformational exchange involving a helical form that is populated in buffer to ~17% for

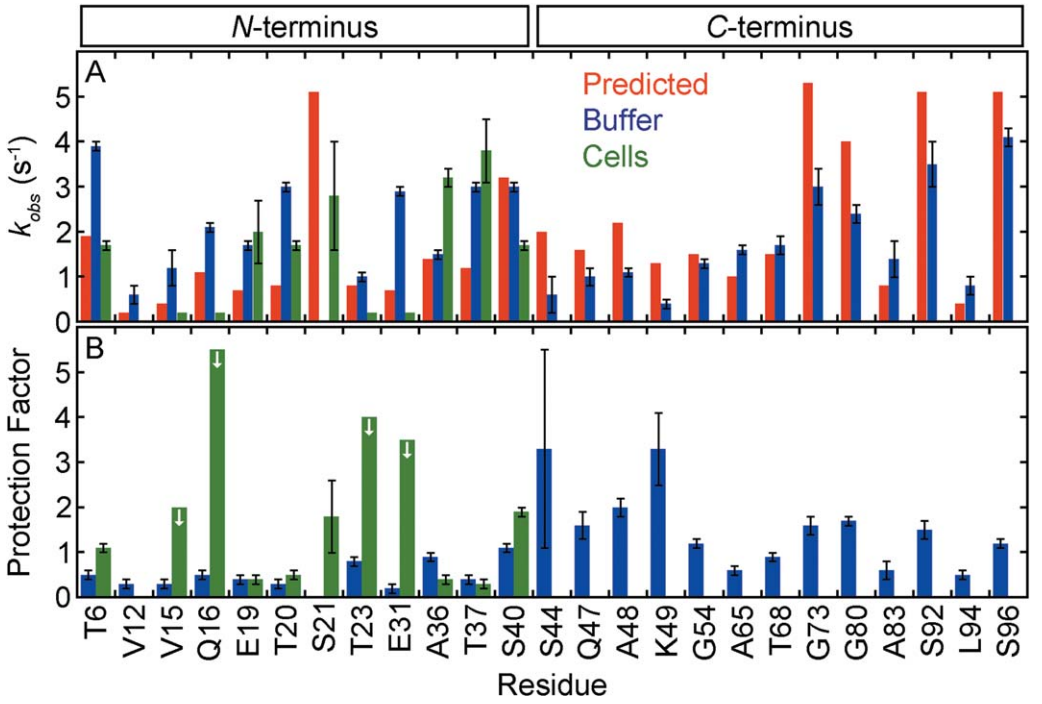

Figure 4. FlgM exhibits similar backbone amide hydrogen exchange rates in cells and in buffer (pH 6.7, 298 K). See the caption to Figure 2 for further information.

acetylated α-synuclein and slightly less for the non-acetylated form.[44,45] This conformational exchange is likely slowed in cells causing broadening. A similar observation has been made for a folding intermediate of the FF domain in cell lysates.[6]

We have shown that measured exchange rates in *E. coli* agree with both those obtained in buffer and those calculated based on exchange rates of small, unstructured peptides. Data for the *C*-terminal region of FlgM in buffer show that even small protection factors can be useful indicators of sparsely populated structured states in disordered proteins. This work also has implications for determining the stability of globular proteins in living cells. Specifically, the data indicate that predicted rates from model peptides can be applied to hydrogen exchange studies of globular proteins inside *E. coli*.[5] Most importantly, we have shown that protein disorder can persist under physiological conditions and that the crowded cellular interior need not affect the structure of disordered proteins.

Materials and Methods

Protein expression for in-cell NMR

Plasmids harboring the gene encoding FlgM (ampicillin resistance) or α-synuclein (ampicillin resistance) were transformed into Agilent BL21 DE3 Gold cells by heat-shock. For acetylated α-synuclein, plasmids harboring pNatB (chloramphenicol resistance) and α-synuclein were co-transformed into Agilent BL21 DE3 Gold cells by electroporation. A single colony was used to inoculate a 5 mL culture of Luria-Bertani media supplemented with 100 μg/mL ampicillin (FlgM or α-synuclein) or 100 μg/mL ampicillin and 25 μg/mL chloramphenicol (pNatB/α-synuclein). The culture was grown at 37°C. After 8 h, 50 μL of the saturated culture was used to inoculate 50 mL of supplemented M9 media as described next.

For uniform labeling, M9 media (50 m*M* Na_2HPO_4, 20 m*M* KH_2PO_4, 9 m*M* NaCl) was supplemented with 2 mg/mL ^{13}C-glucose, 1 mg/mL $^{15}NH_4Cl$, 100 μ*M* $CaCl_2$, 2 m*M* $MgSO_4$, 10 μg/mL thiamine and 10 μg/mL biotin, and 150 μg/mL ampicillin (100 μg/mL ampicillin and 25 μg/mL chloramphenicol for pNatB/α-synuclein). For glycine or threonine "unlabeling," the media described above was also supplemented with 1 mg/mL natural abundance glycine or 1.5 mg/mL natural abundance threonine.[46,47]

For selective lysine/threonine enrichment, natural abundance glucose and NH_4Cl were used in the M9 media, which was also supplemented with 0.1 mg/mL uniformly enriched $^{13}C/^{15}N$ threonine, 0.2 mg/mL uniformly $^{13}C/^{15}N$ enriched lysine and 0.2 mg/mL natural abundance glycine.[48,49]

The 50 mL cultures were shaken (New Brunswick Scientific Innova I26, 225 rpm) at 37°C overnight. The culture was diluted to 100 mL with supplemented M9 media and shaken until the optical density at 600 nm was at least 0.8. Isopropyl β-D-1-thiogalactopyranoside (1 m*M*) was used to induce expression. After 4 h cells were pelleted at 1000*g* and washed 3 times with 30 mL NMR buffer (100 m*M* HEPES, 35 m*M* bis-tris propane,[50] 50 μg/mL chloramphenicol, 100 μg/mL ampicillin, 50% D_2O). For pNatB/α-synuclein the buffer contained half the amount of chloramphenicol and 15 μg/mL rifampin. Chloramphenicol or rifampin are required to halt protein expression prior to NMR. (Rifampin is required because the pNatB plasmid confers chloramphenicol resistance.) Cell pellets were resuspended in 100–200 μL of NMR buffer and loaded into a standard 5 mm NMR tube. Typical cell slurries were 70% wet cells by volume.

Protein purification

Cell pellets were frozen after in-cell NMR experiments. For α-synuclein (with or without acetylation) cells were lysed by boiling. Cell debris was removed by centrifugation at 16,000*g*. Using a GE AKTA FPLC, anion exchange (GE Q column, 50 m*M* Tris wash buffer, 50 m*M* Tris/1*M* NaCl elute buffer, 10–90% gradient) and subsequent size exclusion chromatography (GE Superdex 75 column eluted with non-supplemented M9) were used. Purified protein was dialyzed against 17 MΩ cm^{-1} H_2O for 4 h at room temperature or overnight at 5°C. After dialysis, the sample was flash frozen in a dry-ice/ethanol bath and lyophilized.

FlgM was purified in a similar fashion except the cells were sonicated (Fisher Scientific Sonic Dismembrator Model 500, 15% amplitude, 20 s, 67% duty cycle). FlgM does not bind to anion exchange media.

LC-ESI-MS

Purified samples of α-synuclein were resuspended in 17 MΩ cm^{-1} H_2O and subjected to LC-ESI-MS using a Restek Viva C4 column (linear gradient from 0.1% aqueous formic acid, 5% acetonitrile to 0.1% aqueous formic acid, 95% acetonitrile over 15 m, followed by 5 m in the 95% eluant) coupled to an Agilent 6520 Accurate-Mass Q-TOF running in positive ion mode. Deconvoluted masses of 15240 Da and 15280 Da were found for $^{13}C/^{15}N$ α-synuclein and $^{13}C/^{15}N$ acetylated α-synuclein, respectively. This mass difference corresponds to the addition of an acetyl group (~40 Da). No unmodified α-synuclein was observed when the protein was co-expressed with pNatB, indicating 100% acetylation, consistent with previous work.[51]

pH determination

Purified α-synuclein was suspended in 50 m*M* citrate, 50 m*M* bis-tris propane, 50 m*M* HEPES,

50 m*M* borate, 5% D_2O, containing 0.1% DSS at various pH values. Data were acquired at 288 K (pH: 3.0, 4.2, 5.3, 5.7, 6.0, 6.4, 6.6, 6.8, 7.0, 7.5, 7.8, 8.9) and 298 K (pH: 5.3, 6.1, 6.6, 7.0, 7.4, 7.9, 8.9) on either a 600 or 700 MHz Bruker Avance III HD spectrometer equipped with a Bruker TCI cryoprobe. ^{13}C-HSQC spectra were acquired using sweep widths of 12 ppm in the ^{1}H dimension and 200 ppm in the ^{13}C dimension. Four transients were collected using 512 complex points in t_2 and 64 complex increments in t_1. Spectra were referenced to DSS at 0 ppm. Data were processed with Topspin 3.2. The ^{1}H chemical shifts of H50 $^{13}C^{\epsilon 1}$-^{1}H and $^{13}C^{\delta 2}$-^{1}H of α-synuclein and HEPES were followed as a function of pH. The data were fit to a modified Henderson-Hasselbach equation, $\delta=\delta_{low}-\frac{\delta_{low}-\delta_{high}}{1+10^{n(pKa-pH)}}$, where δ_{low} is the low pH chemical-shift plateau and δ_{high} is the high plateau, n is the number of protons, and pK_a is the negative logarithm of the dissociation constant.[52–54] Our pK_a values (6.7 for H50 and 7.5 for HEPES) are similar to literature values.[39,40]

Using a glass electrode, buffers containing 5% and 50% D_2O and α-synuclein were adjusted to a pH reading of 6.9. The solutions gave nearly identical proton chemical shifts for ε1 (7.984 ppm and 7.983 ppm) and δ2 (7.074 ppm and 7.073 ppm), for 5 and 50% D_2O. Thus, the H50 $^{13}C^{\epsilon 1}$ and $^{13}C^{\delta 1}$ protons are insensitive to the H/D isotope effect and 0.2 pH units were added to the value obtained from the standard curve in solutions containing a 1:1 H_2O:D_2O mixture to account for the H/D isotope effect on the electrode for a 50% D_2O solution.[55,56] The C14 protons of HEPES, however, exhibit an isotope effect. In 5% D_2O the proton chemical shift is 3.117 ppm while in 50% D_2O the chemical shift is 3.134 ppm. For this reason, a correction of −0.017 ppm was applied to values obtained in 50% D_2O to account for the deviation from the conditions used to acquire the standard curve, then the 0.2 pH unit correction was added to the value obtained from the standard curve.

NMR

In-cell samples were prepared as described above. For the buffer experiments purified ^{13}C-, ^{15}N-enriched protein (final protein concentration of ∼500 μ*M* as judged by a Lowry assay using bovine serum albumin as the standard) was added to NMR buffer (pH 6.7, minus antibiotics). One buffer experiment with α-synuclein used NMR buffer plus 150 m*M* NaCl, to ensure minimal salt dependence of exchange. In-cell data were acquired at 288 K (α-synuclein, acetylated α-synuclein), and 298 K (FlgM, α-synuclein) with a 700 MHz Bruker Avance III HD spectrometer running Topspin Version 3.2 and equipped with a Bruker TCI cryoprobe. Buffer data were acquired at 288 K (α-synuclein, acetylated α-synuclein), 293 K (α-synuclein), and 298 K (FlgM, α-synuclein). An interleaved, modified[26] SOLEXSY[29] experiment with mixing times (t_{mix}) of 0, 70, 140, 210, 300, 500, and 800 ms was used to measure hydrogen exchange rates. One in-cell exchange experiment with α-synuclein used t_{mix} of 0, 70, 150, 300, 700 ms in an attempt to shorten the acquisition time and minimize pH changes. Sweep widths were 7000 Hz and 2500 Hz in the ^{1}H and ^{15}N dimensions, respectively. 512 complex points were collected in t_2 with 128 TPPI points in t_1 at each t_{mix}. In buffer, 32 transients were acquired per increment. Forty transients were acquired for the in-cell NMR experiments. Data acquisition required ∼16 h per sample.

^{15}N-^{1}H and ^{13}C-^{1}H HSQC spectra were acquired before and after the SOLEXSY experiment to assess sample integrity and pH. Four or eight transients were collected using 512 complex points in t_2 with 64 complex points in t_1 for each experiment. The sweep widths were 8500 Hz in ^{1}H and either 2500 Hz or 34500 Hz in the ^{15}N or ^{13}C dimension, respectively. For the in-cell samples, the cell slurry was removed after the experiment and gently pelleted. The supernatant was removed, diluted two- to threefold, and placed in the spectrometer. A ^{15}N-^{1}H HSQC was acquired to assess protein leakage.[57] No leakage was observed.

To ensure the pH associated with an in-cell SOLEXSY experiment was the average of the values obtained from the bracketed ^{13}C-^{1}H HSQC spectra, an experiment using α-synuclein was performed where ^{13}C-^{1}H HSQC spectra were acquired as a function of time. These HSQC spectra bracketed a short SOLEXSY (only t_{mix} 0.3 s) experiment and an ^{15}N-^{1}H TROSY-HSQC experiment. This regimen not only allowed us to determine that the pH drop was linear but also allowed collection of single-plane SOLEXSY experiments where the pH drop was only averaged over ∼2.5 h instead of the ∼16 h required for a complete SOLEXSY experiment. This protocol allowed us to assess hydrogen exchange at discreet pH values, instead of exchange averaged over a ∼0.5 pH unit range.

Data processing

Data were processed with NMRPipe.[58] t_2 data were subjected to a cosine squared bell function (512 complex points for buffer solutions and 256 complex points for in-cell experiments) before zero-filling to 2048 points and Fourier transformation. t_1 data were linear predicted to 256 points before application of a cosine squared bell function. Subsequent zero-filling to 1024 points and Fourier transform yielded the final spectra. Spectra were peak picked and integrated using the built-in nlinLS routine. Peak volumes were fitted as described.[29] Published assignments were used.[33,34,59,60]

Acknowledgments

The authors thank Elizabeth Pielak for comments, Eric Brustad and Richard Watkins for help with

mass spectroscopy and Dan Mulvihill for supplying us with the pNatB acetylation complex.

References

1. McGuffee SR, Elcock AH (2010) Diffusion, crowding & protein stability in a dynamic molecular model of the bacterial cytoplasm. PLoS Comput Biol 6:e1000694.
2. Zimmerman SB, Trach SO (1991) Estimation of macromolecule concentrations and excluded volume effects for the cytoplasm of *Escherichia coli*. J Mol Biol 222: 599–620.
3. Zhou HX, Rivas G, Minton AP (2008) Macromolecular crowding and confinement: biochemical, biophysical, and potential physiological consequences. Annu Rev Biophys 37:375–397.
4. Sarkar M, Li C, Pielak GJ (2013) Soft interactions and crowding. Biophys Rev 5:187–194.
5. Monteith WB, Pielak GJ (2014) Residue level quantification of protein stability in living cells. Proc Natl Acad Sci 111:11335–11340.
6. Latham MP, Kay LE (2014) A similar *in vitro* and in cell lysate folding intermediate for the FF domain. J Mol Biol 426:3214–3220.
7. Anfinsen CB (1973) Principles that govern the folding of protein chains. Science 181:223–230.
8. Theillet F-X, Binolfi A, Frembgen-Kesner T, Hingorani K, Sarkar M, Kyne C, Li C, Crowley P, Gierasch LM, Pielak GJ, Elcock AH, Gershenson A, Selenko P (2014) Physicochemical properties of cells and thier effects on intrinsically disordered proteins (IDPs). Chem Rev 114: 6661–6714.
9. Dedmon MM, Patel CN, Young GB, Pielak GJ (2002) FlgM gains structure in living cells. Proc Natl Acad Sci USA 99:12681–12684.
10. Sarkar M, Smith AE, Pielak GJ (2013) Impact of reconstituted cytosol on protein stability. Proc Natl Acad Sci USA 110:19342–19347.
11. Miklos AC, Sarkar M, Wang Y, Pielak GJ (2011) Protein crowding tunes protein stability. J Am Chem Soc 133:7116–7120.
12. Wang Y, Sarkar M, Smith AE, Krois AS, Pielak GJ (2012) Macromolecular crowding and protein stability. J Am Chem Soc 134:16614–16618.
13. Minton AP (2013) Quantitative assessment of the relative contributions of steric repulsion and chemical interactions to macromolecular crowding. Biopolymers 99:239–244.
14. Zhou H-X (2013) Influence of crowded cellular environments on protein folding, binding, and oligomerization: biological consequences and potentials of atomistic modeling. FEBS Lett 587:1053–1061.
15. Luh LM, Hänsel R, Löhr F, Kirchner DK, Krauskopf K, Pitzius S, Schäfer B, Tufar P, Corbeski I, Güntert P, Dötsch V (2013) Molecular crowding drives active Pin1 into nonspecific complexes with endogenous proteins prior to substrate recognition. J Am Chem Soc 135: 13796–13803.
16. Phillip Y, Schreiber G (2013) Formation of protein complexes in crowded environments - From *in vitro* to *in vivo*. FEBS Lett 587:1046–1052.
17. Waudby CA, Camilloni C, Fitzpatrick AWP, Cabrita LD, Dobson CM, Vendruscolo M, Christodoulou J (2013) In-cell NMR characterization of the secondary structure populations of a disordered conformation of α-synuclein within *E. coli* cells. PLoS ONE 8:e72286.
18. McNulty BC, Young GB, Pielak GJ (2006) Macromolecular crowding in the *Escherichia coli* periplasm maintains α-synuclein disorder. J Mol Biol 355: 893–897.
19. Crowley PB, Chow E, Papkovskaia T (2011) Protein interactions in the *Escherichia coli* cytosol: an impediment to in-cell NMR spectroscopy. ChemBioChem 12: 1043–1048.
20. Li C, Charlton LM, Lakkavaram A, Seagle C, Wang G, Young GB, Macdonald JM, Pielak GJ (2008) Differential dynamical effects of macromolecular crowding on an intrinsically disordered protein and a globular protein: implications for in-cell NMR spectroscopy. J Am Chem Soc 130:6310–6311.
21. Englander SW, Kallenbach NR (1983) Hydrogen exchange and structural dynamics of proteins and nucleic acids. Q Rev Biophys 16:521–655.
22. Bai Y, Milne JS, Mayne L, Englander SW (1993) Primary structure effects on peptide group hydrogen exchange. Proteins 17:75–86.
23. Mori S, van Zijl PCM, Shortle D (1997) Measurement of water–amide proton exchange rates in the denatured state of staphylococcal nuclease by a magnetization transfer technique. Proteins: Struct, Funct, Bioinf 28:325–332.
24. Zhang Y-Z. Protein and peptide structure and interactions studied by hydrogen exchange and NMR. In Structural biology and molecular biophysics. University of Pennsylvania, Philadelphia.
25. Connelly GP, Bai Y, Jeng MF, Englander SW (1993) Isotope effects in peptide group hydrogen exchange. Proteins 17:87–92.
26. Smith AE, Sarkar M, Young GB, Pielak GJ (2013) Amide proton exchange of a dynamic loop in cell extracts. Protein Sci 22:1313–1319.
27. Croke RL, Sallum CO, Watson E, Watt ED, Alexandrescu AT (2008) Hydrogen exchange of monomeric α-synuclein shows unfolded structure persists at physiological temperature and is independent of molecular crowding in *Escherichia coli*. Protein Sci 17:1434–1445.
28. Barnes CO, Monteith WB, Pielak GJ (2011) Internal and global protein motion assessed with a fusion construct and in-cell NMR spectroscopy. ChemBioChem 12:390–391.
29. Chevelkov V, Xue Y, Rao DK, Forman-Kay JD, Skrynnikov NR (2010) $^{15}N^{H/D}$-SOLEXSY experiment for accurate measurement of amide solvent exchange rates: application to denatured drkN SH3. J Biomol NMR 46:227–244.
30. Maroteaux L, Campanelli JT, Scheller RH (1988) Synuclein: a neuron-specific protein localized to the nucleus and presynaptic nerve terminal. J Neurosci 8: 2804–2815.
31. Kutsukake K, Iino T (1994) Role of the FliA-FlgM regulatory system on the transcriptional control of the flagellar regulon and flagellar formation in *Salmonella typhimurium*. J Bacteriol 176:3598–3605.
32. Hughes KT, Gillen KL, Semon MJ, Karlinsey JE (1993) Sensing structural intermediates in bacterial flagellar assembly by export of a negative regulator. Science 262:1277–1280.
33. Daughdrill GW, Hanely LJ, Dahlquist FW (1998) The *C*-terminal half of the anti-sigma factor FlgM contains a dynamic equilibrium solution structure favoring helical conformations. Biochemistry 37:1076–1082.
34. Daughdrill GW, Chadsey MS, Karlinsey JE, Hughes KT, Dahlquist FW (1997) The *C*-terminal half of the anti-sigma factor, FlgM, becomes structured when bound to its target, sigma 28. Nat Struct Biol 4:285–291.

35. Serber Z, Corsini L, Durst F, Dötsch V (2005) In-cell NMR spectroscopy. Methods Enzymol 394:17–41.
36. Serber Z, Dötsch V (2001) In-cell NMR spectroscopy. Biochemistry 40:14317–14323.
37. Booth IR (1985) Regulation of cytoplasmic pH in bacteria. Microbiol Rev 49:359–378.
38. Shimba N, Serber Z, Ledwidge R, Miller SM, Craik CS, Dötsch V (2003) Quantitative identification of the protonation state of histidines *in vitro* and *in vivo*. Biochemistry 42:9227–9234.
39. Croke RL, Patil SM, Quevreaux J, Kendall DA, Alexandrescu AT (2011) NMR determination of pKa values in α-synuclein. Protein Sci 20:256–269.
40. Good NE, Winget GD, Winter W, Connolly TN, Izawa S, Singh RMM (1966) Hydrogen ion buffers for biological research. Biochemistry 5:467–477.
41. Ulrich EL, Akutsu H, Doreleijers JF, Harano Y, Ioannidis YE, Lin J, Livny M, Mading S, Maziuk D, Miller Z, Nakatani E, Schulte CF, Tolmie DE, Kent Wenger R, Yao H, Markley JL (2008) Biomagresbank. Nucleic Acids Res 36:D402–D408.
42. Hernández G, Anderson JS, LeMaster DM (2009) Polarization and polarizability assessed by protein amide acidity. Biochemistry 48:6482–6494.
43. Harris DC (2007) Quantitative chemical analysis, 7th ed. W. H. Freeman and Company, New York.
44. Maltsev AS, Ying J, Bax A (2012) Impact of *N*-terminal acetylation of α-synuclein on its random coil and lipid binding properties. Biochemistry 51:5004–5013.
45. Marsh JA, Singh VK, Jia Z, Forman-Kay JD (2006) Sensitivity of secondary structure propensities to sequence differences between α- and γ-synuclein: implications for fibrillation. Protein Sci 15:2795–2804.
46. Shortle D (1994) Assignment of amino acid type in ^{1}H-^{15}N correlation spectra by labeling with ^{14}N-amino acids. J Magn Res 105:88–90.
47. Krishnarjuna B, Jaipuria G, Thakur A, D'Silva P, Atreya H (2011) Amino acid selective unlabeling for sequence specific resonance assignments in proteins. J Biomol NMR 49:39–51.
48. Muchmore DC, McIntosh LP, Russell CB, Anderson DE, Dahlquist FW (1989) Expression and ^{15}N labeling of proteins for proton and ^{15}N nuclear magnetic resonance. Methods Enzymol 177:44–73.
49. Ohki S-y, Kainosho M (2008) Stable isotope labeling methods for protein NMR spectroscopy. Prog Nucl Magn Reson Spectrosc 53:208–226.
50. Kelly AE, Ou HD, Withers R, Dötsch V (2002) Low-conductivity buffers for high-sensitivity NMR measurements. J Am Chem Soc 124:12013–12019.
51. Kang L, Moriarty GM, Woods LA, Ashcroft AE, Radford SE, Baum J (2012) *N*-terminal acetylation of α-synuclein induces increased transient helical propensity and decreased aggregation rates in the intrinsically disordered monomer. Protein Sci 21:911–917.
52. Dyson HJ, Tennant LL, Holmgren A (1991) Proton-transfer effects in the active-site region of *Escherichia coli* thioredoxin using two-dimensional proton NMR. Biochemistry 30:4262–4268.
53. Jeng M-F, Dyson HJ (1996) Direct measurement of the aspartic acid 26 pKa for reduced *Escherichia coli* thioredoxin by ^{13}C NMR Biochemistry 35:1–6.
54. Markley JL (1975) Observation of histidine residues in proteins by nuclear magnetic resonance spectroscopy. Acc Chem Res 8:70–80.
55. Bundi A, Wüthrich K (1979) ^{1}H-NMR parameters of the common amino acid residues measured in aqueous solutions of the linear tetrapeptides H-Gly-Gly-X-L-Ala-OH. Biopolymers 18:285–297.
56. Glasoe PK, Long FA (1960) Use of glass electrodes to measure acidities in deuterium oxide. J Phys Chem 64: 188–190.
57. Barnes CO, Pielak GJ (2011) In-cell protein NMR and protein leakage. Prot: Struct, Funct, Bioinf 79:347–351.
58. Delaglio F, Grzesiek S, Vuister GW, Zhu G, Pfeifer J, Bax A (1995) NMRPipe: a multidimensional spectral processing system based on UNIX pipes. J Biomol NMR 6:277–293.
59. Wu KP, Baum J (2011) Backbone assignment and dynamics of human α-synuclein in viscous 2 M glucose solution. Biomol NMR Assign 5:43–46.
60. Eliezer D, Kutluay E, Bussell R, Browne G (2001) Conformational properties of α-synuclein in its free and lipid associated states. J Mol Biol 307:1061–1073.